# Tidal Wave Propagation in the Flat Basin Under Wind Monsoon Climate

Phan, Hung M.; Reniers, Ad J.H.M.; Stive, Marcel J.F.; Ye, Qinghua

**DOI**
10.1007/978-981-15-2081-5_22

**Publication date**
2020

**Document Version**
Final published version

**Published in**
Estuaries and Coastal Zones in Times of Global Change

**Citation (APA)**
Phan, H. M., Reniers, A. J. H. M., Stive, M. J. F., & Ye, Q. (2020). Tidal Wave Propagation in the Flat Basin Under Wind Monsoon Climate. In K. D. Nguyen, S. Guillou, P. Gourbesville, & J. Thiébot (Eds.), *Estuaries and Coastal Zones in Times of Global Change: Proceedings of ICEC-2018* (pp. 379-388). (Springer Water). Springer. https://doi.org/10.1007/978-981-15-2081-5_22

# Tidal Wave Propagation in the Flat Basin Under Wind Monsoon Climate

**Hung M. Phan, Ad J. H. M. Reniers, Marcel J. F. Stive and Qinghua Ye**

**Abstract** Tide is influenced due to not only mainly tide generating force but also local wind and weather patterns. The East Asian monsoons cause strong seasonal climatic variations in the Mekong Delta. A two-dimensional, barotropic numerical model was employed to investigate the dynamics of tidal wave propagation in the South China Sea with a particular interest for its characteristics along the Mekong deltaic coast under wind monsoon climate. The results reveal that wind monsoon climate could causes damped or amplified tidal amplitudes around Mekong deltaic coast approximately 2–3 cm due to the changing atmospheric pressure, the tangential stress of wind over the water surface, and wind enhanced bottom friction. The monsoon climate influences rather strongly on the $M_2$ semidiurnal tide system in the eastern Mekong deltaic coast, meanwhile the monsoon climate controls $K_1$ diurnal tide in the western region of Mekong delta.

**Keywords** Tidal wave propagation · Wind monsoon climate · Mekong deltaic coast · Delft3D

## 1 Introduction

Tide is the one of fundamental forces influencing hydrodynamic processes and morphology on numerous natural beaches in general as well as Mekong deltaic coast in particular (Fig. 1). Besides mainly tide generating force, tides can also be influenced by local wind and weather patterns. The wind driven contribution to flow and water level changes the tidal amplitude (Wijeratne et al. 2012). The monsoon winds in the South China Sea are caused by the influence of the trade winds and the seasonal change between the location of the earth and the sun. The East Asian monsoons cause strong seasonal climatic variations in the Mekong Delta (Hordoir et al. 2006).

H. M. Phan (✉) · A. J. H. M. Reniers · M. J. F. Stive
Hydraulic Engineering Department, Delft University of Technology, Delft, Netherlands
e-mail: m.h.phan@tudelft.nl

Q. Ye
Software Development Unit, Deltares, Delft, Netherlands



K. D. Nguyen et al. (eds.), *Estuaries and Coastal Zones in Times of Global Change*, Springer Water,
https://doi.org/10.1007/978-981-15-2081-5_22

**Fig. 1** Mekong deltaic coast in Travinh province

Winds are coming mostly from north-east directions in the winter monsoon season from November to April and south-west winds prevail during the summer monsoon. Annual wind speeds have been recorded from 1999 to 2008 by the Southern Regional Hydro-Meteorological Center (Unverricht et al. 2014) at Vung Tau station ranging from 7 to 9 m/s and in Bac Lieu from 6 to 8 m/s. Under stormy conditions wind speeds can reach 20–30 m/s (Institute of Strategy and Policy on natural resources and environment ISPONRE 2009). The maximum wind stress prevails along the south-eastern coast of Vietnam in both monsoon seasons (Unverricht et al. 2014).

Although previous studies (e.g. Wyrtki 1961) agree that the circulation of the SCS is affected mostly by monsoon winds, these studies do not distinguish the different effects between the north east monsoon and the south west monsoon to tidal wave systems. Therefore, it is necessary to clarify the role of wind climate monsoon influencing the tidal wave propagation in the Mekong delta. The mechanisms of tidal wave propagation in the Mekong delta shelf are revealed with the aid of the high-resolution process based model Delft3D.

## 2 Method

### *2.1 Model Set up*

The depth- averaged tidal dynamics model for the whole South China Sea has been constructed using Delft3D-FLOW, which includes the shallow water equations, the continuity equations and the transport equations for conservative constituents. This

model ranges from 96°–126°E and from 8°S to 24°N with flexible orthogonal mesh features with grid cell sizes nearly 22 km near the offshore boundaries and gradually reducing to 4 km around Mekong deltaic coast. The finer grids are necessary to resolve the topography needed for an accurate simulation. A total of 8 primary tidal constituents (O1, K1, P1, Q1, M2, S2, K2, N2) derived from 15 years of Topex-Poseidon and Jason-1 satellite altimetry (Gerritsen et al. 2003) adjusted to GMT 7 + have been applied for tidal simulations at 8 main boundaries, viz. Taiwan Strait, Luzon Strait, Celebes Zee, Flores Zee, Sape Strait, Lombok Strait, Sunda Strait and Andaman Zee.

The bathymetry data shown in Fig. 2a are obtained, from the General Bathymetric Chart of the Oceans (GEBCO) bathymetry database with 30 arc-second grid resolution. Higher resolution bathymetry data along Mekong deltaic coast are obtained by a bathymetry survey of the Mekong deltaic coast in 2009 and 2010 in the context of a Vietnam Government project (SIWRR 2010). The bed friction coefficient is $0.026\ m^{-1/3}$ s globally with some local values of $n = 0.015\ m^{-1/3}$ s on the Vietnamese shelf and a value of $n = 0.5\ m^{-1/3}$ s across the archipelagos separating the Sulu Sea from the South China Sea and the Celebes Sea accounting for the effect of partly unresolved islands and underwater ridges. As the model domain covers a large area and the water depth of several sections is relatively deep, TGF are included in this model and calculated including the equilibrium tide and the earth tide. In the model, the TGF of 10 tidal constituents (M2, S2, N2, K2, K1, O1, P1, Q1, MF, and MM) are considered. The six branches of the Mekong River are included as river boundaries with hourly discharges. The value for the horizontal eddy viscosity depends on the flow and the grid size used in the simulation. Because of the large area with grid sizes of kilometers, the horizontal eddy viscosity is specified at 250 $m^2/s$ (Gerritsen et al. 2003). wind data available from NOAA.

## 2.2 Model Results Validation

The simulation is carried out for the whole year of 2014 using a time step of 5 min at zero initial conditions. In the whole South China Sea, along the coast of the Mekong Delta on the southern Vietnam shelf, 41 tidal stations were selected for model verification. Practical error measures for a tidal constituent k are the summed vector difference and root mean square error over selected observations:

$$SVD_k = \sum_{s=1}^{s=s\max} VD_{k,s}$$

$$VD_{k,s} = \sqrt{(H_{c,k}\cos G_{c,k} - H_{o,k}\cos G_{o,k})^2 + \left(H_{c,k}\sin G_{c,k} - H_{o,k}\sin G_{o,k}\right)^2}$$

where $H_{c,k}, G_{c,k}, H_{o,k}, G_{o,k}$ are the computed and observed astronomical amplitude and phase of a tidal constituent k.

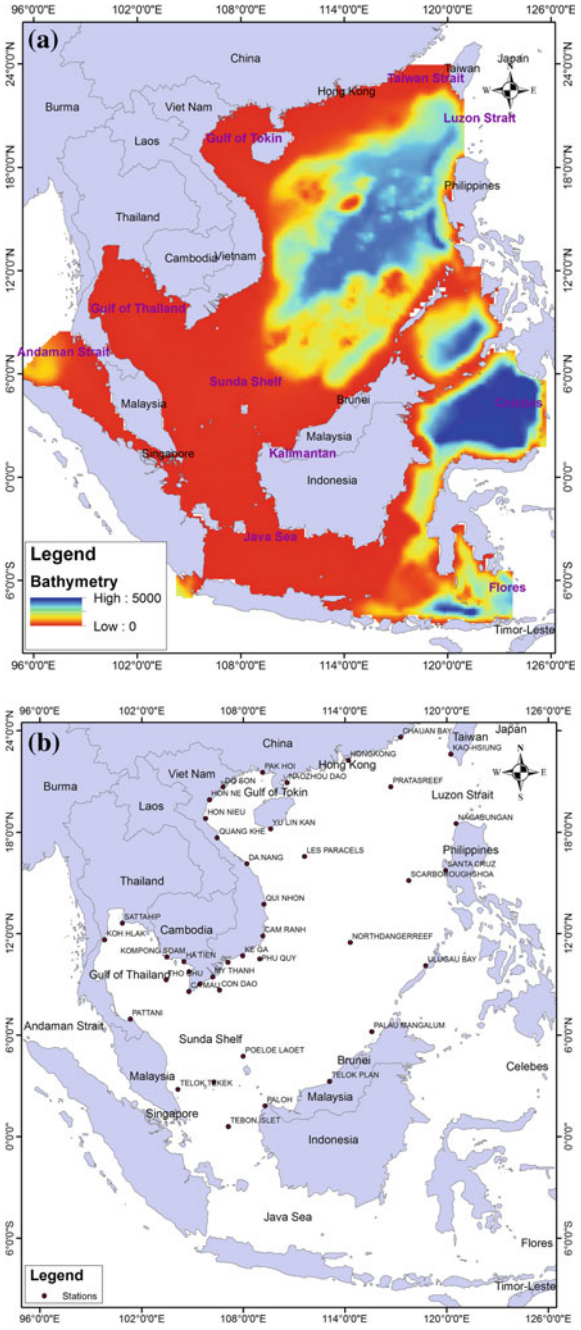


**Fig. 2** **a** Bathymetry and **b** tidal data stations in the South China Sea

The RMSE of the complex amplitude is $\sqrt{\frac{1}{2N}\sum_{i=1}^{N}|H_{Si}-H_{Oi}|^2}$

where N is the number of the observation stations; $H_{Si}$ and $H_{Oi}$ are the model simulated and observation amplitude at station i, respectively.

Computed astronomical amplitudes and phases are analysed by a tidal harmonic analysis program called Delft3D-TIDE tool. The astronomical tide observed in oceans and seas is directly or indirectly the result of gravitational forces acting between the sun, moon, and earth. The influence of other celestial bodies is negligibly small. The observed tidal motion can be described in terms of a series of simple harmonic constituent motions, each with its own characteristic frequency l (angular velocity). The amplitudes A and phases G of the constituents vary with the positions where the tide is observed. The general formula for the astronomical tide is:

$$H(t) = A_0 + \sum_{i=1}^{k} A_i F_i \cos(w_i t + (V_0 + u)_i - G_i$$

Where: H(t): water level at time t; $A_0$: mean water level over a certain period; K: number of relevant constituents; I: index of a constituent; $A_i$: local tidal amplitude of a constituent; $F_i$: nodal amplitude factor; $W_i$: angular velocity; $(V_0 + u)_i$: astronomical argument; $G_i$: improved kappa number (=local phase lag).

The Delft3D-TIDE tool is formulated in terms of k relevant constituents, a total of (2 k +1) unknowns A0, Ai and Gi must be determined (or (2 k +2) unknowns, if Bt is included). This is realised by minimisation of the quantity: $\sum(W(t) - H(t))^2$ using a least—squares technique.

The harmonic constants of water level from 41 observation stations shown in Fig. 2b are collected from the International Hydrographic Organization (IHO) tidal dataset, published papers by Fang et al. (1999), Zu et al. (2008), permanent stations of Vietnam southern regional hydrometeorological center as well as the Global Tide Model. The Global Tide Model is developed by DTU Space (DTU10). The Global Tide Model is available on a 0.125 × 0.125 degree resolution grid for the major 10 constituents in the tidal spectra. This model is utilizing the latest 17 years multi-mission measurements from TOPEX/Poseidon, Jason-1 and Jason-2 satellite altimetry. The computed and observed harmonic constants are listed together for comparison (Fig. 3).

## 3 Results and Discussion

While climate seasonality is produced by the tilting of the Earth, monsoon climate systems are a consequence of the land-sea temperature differences affected by solar radiation (Huffman et al. 1997). The monsoon climate is an atmospheric flow over Asia and is variable greatly depending on the Siberian High and the Arctic Oscillation (Wang et al. 2012). The Southeast Asia countries are controlled by the monsoon climate, which is a large-scale seasonal reversals of the wind system (Serreze

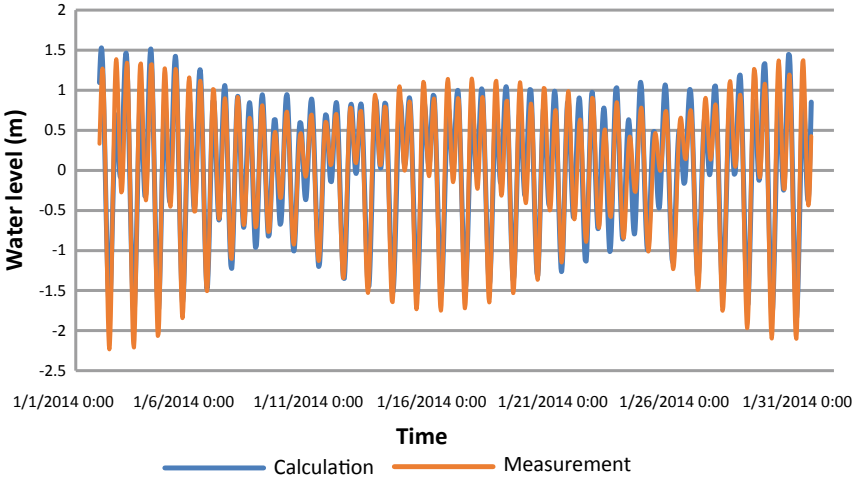


**Fig. 3** Calculated and measured water level at Vungtau station

et al. 2010). The two main monsoon regimes are specifically named the northeast monsoon (winter monsoon) from November to April and the southwest monsoon (summer monsoon) from late May to September. Furthermore, October is the transition month from the southwest to northeast monsoon seasons (Cruz et al. 2012). The summer monsoon occurs when rainfall touches maximum during the boreal winter, whereas the winter monsoon takes place during boreal summer where rainfall reaches maximum.

Fluctuations of sea level are superimposed upon regular tidal oscillations. In addition to the temporary and often dramatic variations in sea level due to tsunamis, hurricanes and other storms, variations in the predicted sea level frequently occur in association with the regular path of cyclonic disturbances across the coastal waters. These changes in sea level may be attributed in part to modifications to the changing atmospheric pressure and in part to the build-up or reduction of water at the coast due to the tangential stress of wind over the water surface. The pressure gradients in the horizontal momentum equations for water of constant density (Deltares 2014) are computed by:

$$\frac{1}{\rho}P_x = g\frac{\partial \zeta}{\partial x}, \quad \frac{1}{\rho}P_y = g\frac{\partial \zeta}{\partial x}$$

where in ρ are the density of water, respectively, Px and Py are the horizontal pressure terms in the Cartesian horizontal x, y direction, ζ is water level above some horizontal plane of reference, g is acceleration due to gravity.

The steady state effect of wind stress on the free surface, wind is implemented as a uniform shear stress, based on the wind data available shown in Fig. 4 from NOAA included in the momentum equations. Wind stress magnitudes (Deltares 2014) are

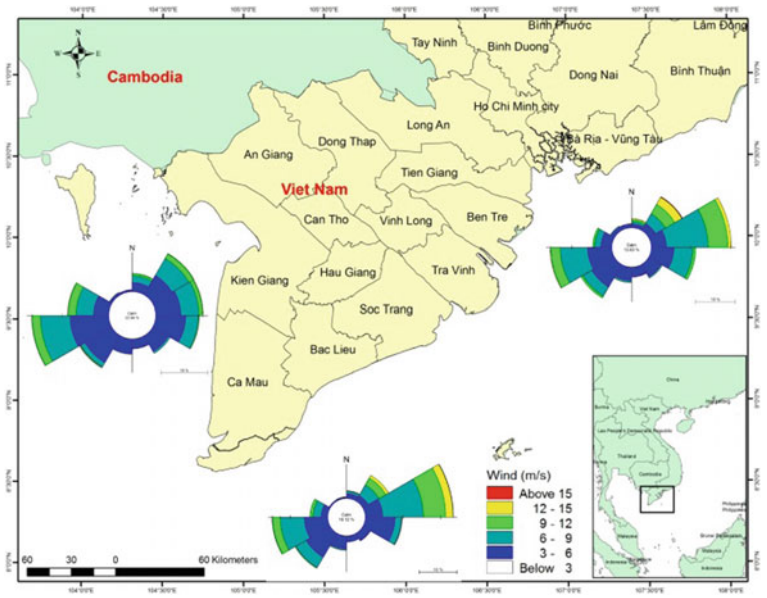


**Fig. 4** Wind rose maps in Mekong deltaic coast

computed by:

$$\left|\overrightarrow{\tau_w}\right| = \rho_\alpha C_d U_{10}^2$$

where in $\rho_\alpha$ is the density of air (kg/m3), $U_{10}$ the wind speed 10 m above the free surface (m/s) and $C_d$ the wind drag coefficient.

Besides, Ruessink et al. (2006) showed that wind driven flow enhanced friction during the flood phase of a tidal cycle more than it reduced friction during the ebb flow, thereby increasing the friction over the tidal cycle and reducing the tide current range. Jones and Davies (2008) showed that changes in the bottom stress affect tidal elevations and currents in shallow sea during prevailing wind. The bed stress ((τ_b) $^{\rightarrow}$) is modeled as a quadratic friction based on the magnitude of the Eulerian velocity in the first layer above the bed ((u_b) $^{\rightarrow}$) (Deltares 2014):

$$\overrightarrow{\tau_b} = \frac{g\rho_0 \overrightarrow{u_b}\left|\overrightarrow{u_b}\right|}{C_{2D}^2}$$

where C2D is the 2D-Chézy coefficient (based on calibration of water levels), ρ_0is the density of water body.

Figure 5a, b show the difference of M2 semidiurnal tidal amplitudes and co-phase lines between original condition and wind climate monsoon condition. The results in the winter monsoon climate show that atmospheric forcing attenuates the M2 tidal amplitude up to 2.5 cm at Soc Trang province on the eastern Mekong deltaic coast,

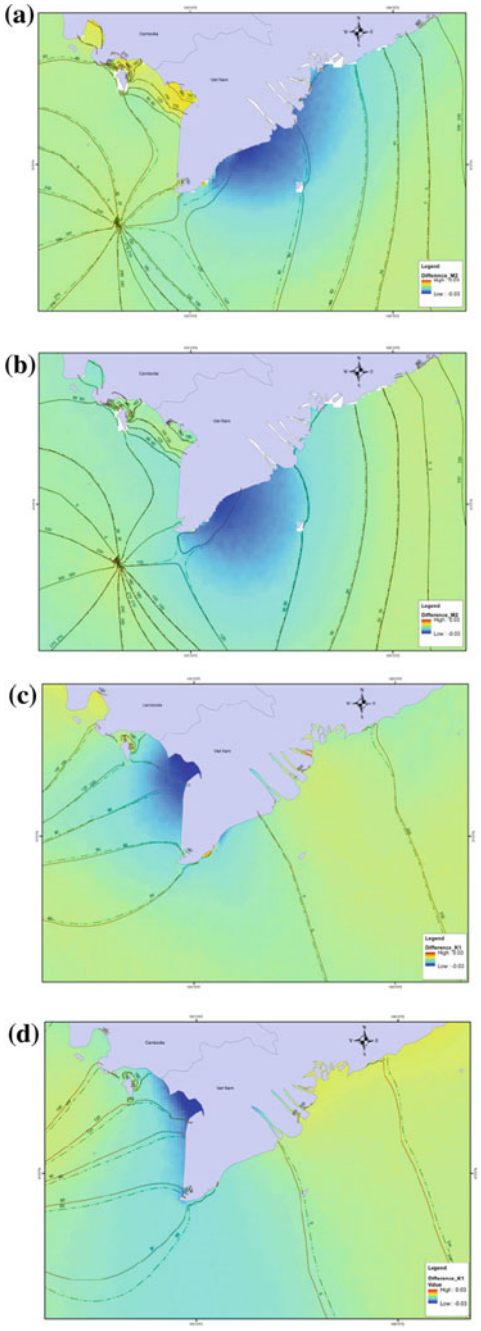


**Fig. 5** Phase and amplitude difference of M2, K1 in case of wind climate monsoon in winter **a**, **c** summer **b**, **d**, brown and green lines represent the co-phase lines of case original condition and case of wind climate monsoon

meanwhile the difference of M2 tidal phase is insignificant only 3–4 min. In the summer monsoon, the M2 tidal amplitude is similarly damped until roughly 2 cm by wind forcing from a dominant southwest direction. The intensity of the M2 tidal amplitude attenuation in the summer monsoon moves southward compared with the winter monsoon as a result of distributive spatial difference of wind strength and atmospheric pressure in the climate monsoon.

Similarly, the change of the K1 semidiurnal tidal amplitudes and co-phase lines between the original condition and the wind climate monsoon condition are shown in Fig. 5c, d. Different from the M2 semidiurnal tide, the K1 diurnal tide is attenuated by an average of 1–2 cm in the western Mekong deltaic coast due to the distribution of tidal characteristic in around Mekong deltaic coast. The largest damped K1 diurnal amplitude amounts to 2.5–2.6 cm along the Kiengiang coast in both the winter and summer monsoon climate. Like for the M2 tide, the difference of K1 tidal phases is minor, i.e. only 8–10 min. Therefore, the influence of wind climate monsoon through the wind stress on the surface as well as the bed stress varies from region to region. The monsoon climate influences rather strongly on semidiurnal tide in the eastern Mekong deltaic coast, inversely the diurnal tide is affected quite considerably by the monsoon climate in the western region of Mekong delta.

## 4 Conclusion

A two-dimensional tidal model is constructed with a high resolution to allow the simulation of accurate tidal wave propagation in the South China Sea as well as along the Mekong deltaic coast under wind monsoon climate. The effect of the wind monsoon climate to the tidal wave system in this flat basin is investigated. The results reveal that atmospheric forcing in the monsoon climate could cause damped or amplified tides along the Mekong deltaic coast. The monsoon climate influences rather strongly on the $M_2$ semidiurnal tide system in the eastern Mekong deltaic coast, meanwhile the monsoon climate controls $K_1$ diurnal tide in the western region of Mekong delta.

## References

Cruz, F. T., Narisma, T. G., Villafuerte, M. Q., Cheng, K. U. C., & Olaguera, L. M. (2012). A climatological analysis of the southwest monsoon rainfall in the Philippines. *Atmospheric Research, 122*(2012), 609–616.

Deltares (2014). User manual, Delft3D Flow, Deltares, Delft, the Netherlands.

Fang, G., Kwok, Y. K., Yu, K., & Zhu, Y. (1999). Numerical simulation of principal tidal constituents in the South China Sea, Gulf of Tokin and Gulf of Thailand. *Continental Shelf Research, 19,* 845–869.

Gerritsen, H., Schrama, E. J. O., Van der Boogaard, H. F. P. (2003). Tidal model validation of the seas of South East Asia using altimeter data and adjoint modelling. In *Proceedings of the 30th IAHR Congress*, Thessaloniki (Vol. D, pp. 239–246).

Hordoir, R., Polcher, J., Brun-Cottan, J.-C., & Madec, G. (2006). Towards a parametrization of river discharges into ocean general circulation models: A closure through energy conservation. *Climate Dynamics, 31*(7–8), 891–908.

Huffman, G. J., Adler, R. F., Arkin, P., Chang, A., Ferraro, R., Gruber, A., et al. (1997). The Global Precipitation Climatology Project (GPCP) combined precipitation dataset. *Bulletin of the American Meteorological Society, 78,* 5–20.

Institute of Strategy and Policy on natural resources and environment (ISPONRE). (2009). *Vietnam Assessment Report on Climate Change.* 127.

Jones, JE., Davies, AM. (2008) On the modification of tides in shallow water regions by wind effects. *Journal of Geophysical Research, 113* (C5).

Ruessink, B. G., Houwman, K. T., Grasmeijer, B. T. (2006) Modeling the nonlinear effect of wind on rectilinear tidal flow. *Journal of Geophysical Research-Oceans, 111*(C10002). http://dx.doi.org/10.1029/2006JC003570.

Serreze, R. G., Barry, R. G., and Chorley, R. J. (2010). *Atmosphere, Weather and Climate.* Routledge, Oxon.

Southern Institute of Water Resources Research (SIWRR). (2010). *Project for measurements of bathymetry, hydrodynamics in estuaries and coastal zone of Mekong delta from 2009 to 2010*. http://www.siwrr.org.vn/?id=nckh5 (in Vietnamese).

Unverricht, D., Nguyen, T. C., Heinrich, C., Szczucinski, W., Lahajnar, N., & Stattegger, K. (2014). Suspended sediment dynamics during the inter-monsoon season in the subaqueous Mekong Delta and adjacent shelf, southern Vietnam. *Journal of Ansian Earth Sciences, 79,* 509–519.

Wang, L., Li, J., Lu, H., Gu, Z., Rioual, P., Hao, Q., et al. (2012). The East Asian winter monsoon over the last 15,000 years: Its links to high-latitudes and tropical climate systems and complex correlation to the summer monsoon. *Quaternary Science Reviews, 32,* 131–142.

Wijeratne, E. M. S., Pattiaratchi, C., Eliot, M., & Haigh, I. D. (2012). Tidal characteristics in Bass Strait, south–east Australia. *Estuarine Coastal and Shelf Science, 114,* 156–165.

Wyrtki, K. (1961). *Physical oceanography of the Southeast Asian waters*. Scientific Results of Marine Investigations of the South China Sea and the Gulf of Thailand 1959–1961 (NAGA Report. 2). La Jolla, California: Scripps Institution of Oceanography, P. 195.

Zu, T., Gan, J., & Erofeeva, S. Y. (2008). Numerical study of the tide and tidal dynamics in the South China Sea. *Deep Sea Research I, 55,* 137–154.